BEC and Optical Lattices

Dieter Jaksch

Clarendon Laboratory
University of Oxford

Bibliography

- Bose-Einstein condensation by L. Pitaevskii and S. Stringari
- Bose-Einstein condensation in Dilute Gases by C.J. Pethick and H. Smith

Contents

1 Introduction

Bose–Einstein condensation (BEC) predicted by Einstein [1] and Bose [2] in 1924 was first observed in alkali atomic vapors in 1995. In contrast to much older experiments with Helium where strong interactions between the particles wash out most of the effects expected in a BEC the relatively weak two–particle interaction in dilute alkali gases allows the study of properties of BEC experimentally. Those experiments and the possibility of a theoretical description of weakly interacting bosonic systems starting from fundamental quantum mechanics has stimulated a lot of experimental and theoretical effort towards a deep understanding of BEC.

After the first experiments in 1995 had shown clear evidence of BEC the following ones concentrated on investigating the properties of condensates. BEC has led to a better understanding of ultracold collisions between neutral atoms. It allows the determination of the s–wave scattering length with a very high accuracy [3] and it was also possible to study Feshbach resonances by applying external magnetic fields [3]. Also, studies of inelastic two– and three–particle processes [4] were done in BEC. Even interactions between mixtures of Bose–condensates of different species of atoms [5, 6] as well as the coherence properties and relative phases of these binary mixtures [7] have been studied experimentally. Furthermore a lot of effort has been put in measuring collective excitations and phonon modes [8], the sound velocity [9], the structure factor [10], the properties of particles coupled out of a condensate [11], and the initiation of the condensation process [12]. By stirring or rotating a BEC quantized vortices [13] were experimentally created and their properties investigated in detail. It was even possible to achieve vortex lattices [14] as shown in Fig. 1.

From 1999 the research on ultracold matter was boosted by first successful experiments on loading BECs into optical lattices [15]. Optical lattices are created by the AC-Stark shift caused by interfering laser beams and produce periodic trap potentials for the BEC atoms. The trap parameters defined by an optical lattice can be controlled in a very wide range by the laser parameters yielding a versatile trap geometry [16]. Optical lattices are ideally suited to produce and study one and two dimensional BECs with the remaining degrees of freedom frozen out. They also allow to alter the ratio of kinetic to interaction energy significantly with respect to magnetically trapped BEC which led to a seminal experiment by M. Greiner [17] where an optical lattice was used to adiabatically transform a BEC into a Mott insulating (MI) state. While a BEC state is characterized by off-diagonal coherence over the whole size of the BEC an MI state has a commensurate filling of lattice sites and does not show off-diagonal coherence and consequently there are no particle number fluctuations. Experimentally vanishing of off-diagonal coherence leads to vanishing interference fringes in the density profile after the particles are released from the trap as shown in Fig. 2.

The advanced control over ultracold trapped bosonic atoms have led to a number of applications. They enabled experimentalists to extend their efforts from bosonic alkali atoms to fermionic systems and even molecules. Starting from an atomic BEC molecules can be created either by using Feshbach resonances [18] or by photoassociation [19]. Recently, BECs have also been used successfully to sympathetically cool Fermigases [20] of weakly interacting atoms into their degenerate regime. Ultracold neutral atoms can be used to study entanglement and for quantum information processing [21, 22]. Condensates can be exploited for building a coherent source of neutral atoms as shown in [11]. In summary, the creation of BEC has become a standard task for experimentalists within the last few years. BECs have become common tools of experimental atomic and molecular physics and are used in many experiments on ultracold matter.

By using the Gross–Pitaevskii equation (GPE) [23] one can study most of the properties of

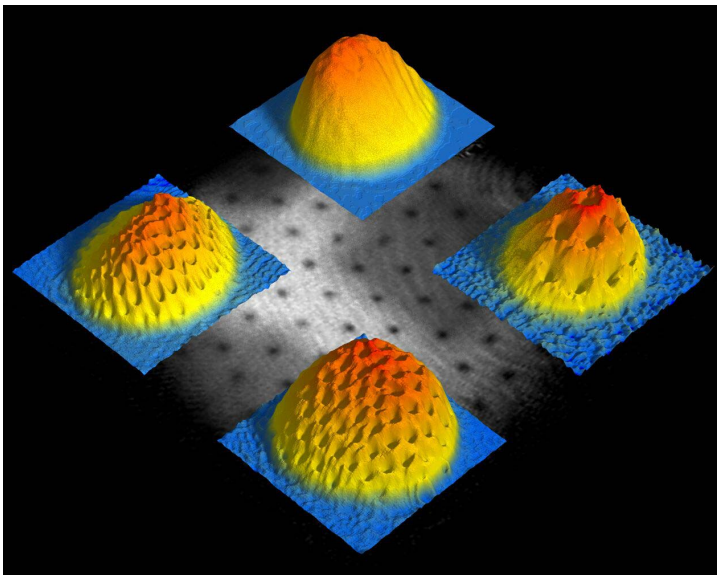

Figure 1: Vortex lattice in a BEC.

a weakly interacting condensates theoretically. The GPE describes trapped weakly interacting many particle bosonic systems by means of a macroscopic wavefunction at temperature $T = 0$. The two–particle interaction potential is approximated by a contact potential and characterized by the s–wave scattering length [24]. Depletion of the condensate [25], which becomes important in strongly interacting systems, is neglected. The GPE also does not include thermal fluctuations of the condensate. Although the approximations leading to the GPE seem rather severe many of the macroscopic quantum mechanical effects that become visible in BEC experiments can be described well by using the GPE.

The relative phase of a condensate used to describe interference between BECs has been investigated in [26], theoretical studies on vortices and various other topological effects in a BEC can be found in [27] and BECs with two or more components have been studied in [28]. Furthermore most of the theoretical work done on ultracold collisions [29] is in good agreement with the experiments. Mean field theories that describe BEC at finite temperature have been developed in [30, 31, 32]. The most powerful method to describe a BEC at finite temperature is quantum kinetic theory which we will not discuss further here. Also the initiation of BEC is well understood by using quantum kinetic theory. For BECs loaded into an optical lattice the GPE and mean field theory may break down. An accurate model of this situation is provided by the Bose-Hubbard Hamiltonian [16] which allows to treat the BEC as well as the MI limit.

We will now look at the most important properties of BECs. The overview given here cannot be complete, it is merely a collection of some of the most important results and a list of references. The reference include review articles considering different aspects of recent research on cold atom physics in more detail [33, 34, 35].

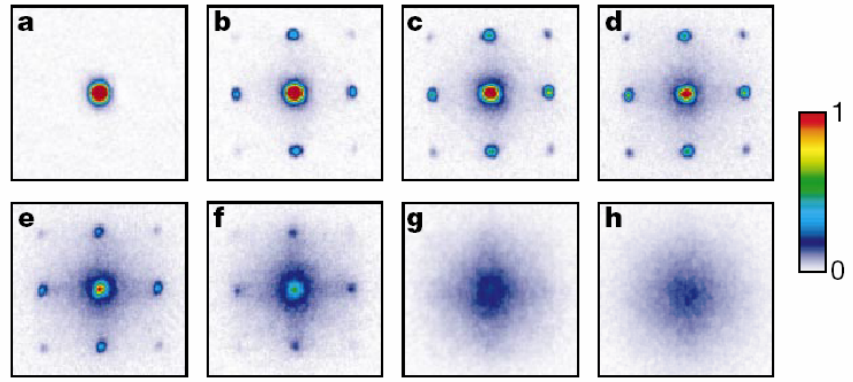

Figure 2 Absorption images of multiple matter wave interference patterns. These were obtained after suddenly releasing the atoms from an optical lattice potential with different potential depths V_0 after a time of flight of 15 ms. Values of V_0 were: **a**, 0 E_r; **b**, 3 E_r; **c**, 7 E_r; **d**, 10 E_r; **e**, 13 E_r; **f**, 14 E_r; **g**, 16 E_r; and **h**, 20 E_r.

Figure 2: Inteference patterns of particles released from an optical lattice

2 BEC of an ideal Bose–gas in a trap

In this section we briefly present the basic properties of a trapped ideal bosonic gas in thermodynamic equilibrium. We investigate a Bose–gas at temperature $T = 0$ and then extend the desciption to finite temperatures.

2.1 Ideal Bose gas at zero temperature

2.1.1 Hamiltonian

The second quantized Hamiltonian $H_{\rm id}$ of a trapped non–interacting Bose gas is given by

$$H_{\rm id} = \int d^3x\, \Psi^\dagger(\mathbf{x}) \left(\frac{\mathbf{p}^2}{2m} + V_T(\mathbf{x}) \right) \Psi(\mathbf{x}), \tag{1}$$

where $\mathbf{x}$ is the coordinate space operator, $\mathbf{p}$ is the momentum operator and m denotes the mass of the particles. $\Psi(\mathbf{x})$ is the bosonic field operator obeying the usual bosonic commutation relations

$$\left[\Psi(\mathbf{x}), \Psi^\dagger(\mathbf{x}') \right] = \delta(\mathbf{x} - \mathbf{x}'). \tag{2}$$

The trapping potential is denoted by $V_T(\mathbf{x})$.

2.1.2 Eigenstates

In the non–interacting case it is most convenient to choose the eigenstates of the one particle Hamiltonian

$$H_1 = \frac{\mathbf{p}^2}{2m} + V_T(\mathbf{x}), \tag{3}$$

as the set of mode functions for describing the many particle system. The eigenfunctions of H_1 are written as $\phi_i(\mathbf{x})$, and the corresponding eigenvalues are ϵ_i. We will assume $\epsilon_i \leq \epsilon_j$ for $i < j$ and i, j to be positive integers. The eigenstates of the many particle system are written as

$$|\psi\rangle = |n_0, n_1, ..., n_i, ...\rangle \,, \tag{4}$$

where the n_i give the number of particles occupying the one particle mode ϕ_i. The state of the system is uniquely defined by $|\psi\rangle$ since the bosonic particles are indistinguishable [36].

2.1.3 Ground state

At temperature $T = 0$ the system is in its ground state. Since in the case of bosons quantum statistics does not forbid an arbitrary number of particles to occupy a single one–particle state [36] the ground state is immediately found to be given by

$$|\psi_0\rangle = |N, 0, 0, ...\rangle \,, \tag{5}$$

where N is the number of particles in the system. All N particles occupy the same one particle state in this case, i.e. a *macroscopic* number of particles show the *same quantum properties*. This can be viewed as a macroscopic manifestation of quantum mechanics.

2.2 What is a Bose–Einstein condensate?

A Bose–Einstein condensate is defined to be a macroscopic number of bosons that occupy the same one–particle state [37] at a finite temperature $T > 0$. Given the density operator ρ of a bosonic system one can find out whether the Bose–gas is condensed by diagonalizing the one particle density operator ρ_1 which is defined by

$$\rho_1 = \mathrm{Tr}_{\,2,...,N} \rho, \tag{6}$$

where $\mathrm{Tr}_{\,2,...,N}$ denotes the trace over particles 2 to N. If one finds an eigenvalue N_c (belonging to the mode function $\phi_c(\mathbf{x})$) which is of the order of the total number of particles N in the system then N_c particles are said to be condensed in the mode function $\phi_c(\mathbf{x})$. Note that in an ideal Bose gas at $T = 0$ all particles occupy the single particle mode function $\phi_0(\mathbf{x})$, however, in the case of an interacting Bose–gas even at $T = 0$ not all the particles are condensed. Then no set of mode functions exists where the ground state of the system can be written as $|\psi_0\rangle = |N, 0, 0, ...\rangle$ [25].

2.3 Thermodynamic properties

We discuss the thermodynamic properties of a trapped ideal bosonic gas in the grand canonical ensemble. A detailed comparison of the behavior in the grand canonical, canonical, and micro canonical ensemble can be found in [38].

2.3.1 Trapped ideal bose gas in the grand canonical ensemble

For simplicity we assume $V_T(\mathbf{x})$ to be harmonic and isotropic, i.e. $V_T(\mathbf{x}) = m\omega\mathbf{x}^2/2$, where ω is the trap frequency. A system in the grand canonical ensemble is assumed be interacting with a heat bath and allowed to exchange particles with a particle reservoir. The density operator in thermal equilibrium is given by

$$\rho_G = \frac{1}{Z_g} e^{-\beta(H_{\mathrm{id}} - \mu\hat{N})}, \tag{7}$$

where $\beta = 1/kT$ is the inverse temperature,

$$\hat{N} = \int d^3x \Psi(\mathbf{x})^\dagger \Psi(\mathbf{x}) \tag{8}$$

is the number operator, and μ, the chemical potential, fixes the mean number of particles N in the system. Setting the ground state energy equal to zero we find the grand canonical partition function defined by

$$Z_g = \mathrm{Tr}\left\{e^{-\beta(H_{\mathrm{id}} - \mu\hat{N})}\right\}, \tag{9}$$

to be given by

$$Z_g = \prod_{j=0}^{\infty} \left(\frac{1}{1 - Ze^{-\beta\hbar\omega j}}\right)^{\frac{(j+1)(j+2)}{2}}, \tag{10}$$

where $Z = \exp(\beta\mu)$ is the fugacity. The mean number of particles in the system is given by

$$N = \sum_j \frac{(j+1)(j+2)}{2} n_j, \tag{11}$$

where n_j is the number of particles in a one particle state with energy $\epsilon_j = \hbar\omega j$ given by

$$n_j = \frac{1}{Z^{-1}e^{\beta\hbar\omega j} - 1}. \tag{12}$$

Approximating the sum Eq. (11) by an integral and treating the ground state separately [36] we find

$$N = n_0 + \frac{g_3(Z)}{(\beta\hbar\omega)^3}, \tag{13}$$

where $n_0 = Z/(1-Z)$ and $g_3(Z)$ is the Bose–function

$$g_3(Z) = \frac{1}{2}\int_0^\infty \frac{x^2}{Z^{-1}e^x - 1}. \tag{14}$$

Thus in the thermodynamic limit $N \to \infty$, $\omega \to 0$ and $\omega^3 N = \text{const.}$ we find

$$\frac{n_0}{N} = \begin{cases} 1 - \left(\frac{T}{T_c}\right)^3 & \text{for} \quad T < T_c \\ 0 & \text{for} \quad T \geq T_c \end{cases}, \tag{15}$$

where the critical temperature T_c is defined by

$$kT_c = \hbar\omega \left(\frac{N}{\zeta(3)}\right)^{1/3}, \tag{16}$$

with $\zeta(3) = g_3(1)$ the Riemann–zeta function. We do not want to go into the details on how to find the fluctuations in the grand canonical system since these can be found in [36].

The results obtained in the grand canonical ensemble agree rather well with current experiments as long as no fluctuations are being calculated. Since in experimental setups no particle reservoir is at thermal equilibrium with the Bose–gas the huge particle number fluctuations predicted by the grand canonical ensemble for particles in the ground state do not emerge in the experiment.

3 BEC of the weakly interacting Bose–gas

Even in dilute alkali Bose–gases as used in current BEC experiments two particle interactions must not be neglected since they strongly influence the behavior of the Bose–gas. Some of the interesting properties of Bose–Einstein condensates determined by the interaction are

- the formation of a BEC [39],
- the shape of the BEC mode function [23],
- collective excitations of a BEC [40],
- the quasiparticle spectrum [40],
- and the domain structure of two species BECs [28].

Also the evaporative cooling mechanism is based on the elastic thermalizing collisions between two particles [41].

3.1 Two–particle interaction

The Hamiltonian of two interacting particles (without external trap potential) is given by

$$H_{\text{int}} = \frac{\mathbf{p}_1^2}{2m} + \frac{\mathbf{p}_2^2}{2m} + V\left(\mathbf{x}_1 - \mathbf{x}_2\right) \tag{17}$$

where $\mathbf{p}_i$ and $\mathbf{x}_i$ are the momentum and the coordinate space operators of particle $i = 1, 2$, respectively. $V\left(\mathbf{x}_1 - \mathbf{x}_2\right)$ is a short range potential with an s–wave scattering length denoted by a_s usually of the order of a few Bohr radii a_0 [3]. BEC experiments are commonly performed in the limit where the thermal wave–length λ_T is much larger than the scattering length a_s. Thus only s–wave scattering with a relative wave vector between the two particles k much smaller than the inverse of the scattering length $1/a_s \gg k$ will be important. Outside the range of the interaction potential its effect on s–waves is the same as if the potential was a hard sphere potential with radius a_s [24]. The effect of a hard sphere potential is nothing more than a boundary condition for the relative wave function of the two particles at $r = a_s$ (with $\mathbf{r} = \mathbf{x}_1 - \mathbf{x}_2$). As shown by K. Huang in [24] this boundary condition can be enforced by replacing the interaction potential by a pseudo–potential of the form

$$V\left(\mathbf{x} - \mathbf{x}'\right) \to \frac{4\pi a_s \hbar^2}{m} \delta\left(\mathbf{x} - \mathbf{x}'\right). \tag{18}$$

Note that this replacement yields correct results only for the wave function outside the range of the actual interaction potential and thus the wave function of the relative motion has to extend over a space with volume much larger than a_s^3. Otherwise measurable quantities will strongly depend on the form of the wave function within the range $r < a_s$ where the pseudo–potential approximation is not valid. In the many body case this condition is only satisfied if the mean distance between the particles is much larger than the range of the interaction potential, i.e.,

$$\eta = n a_s^3 \ll 1, \tag{19}$$

where n is the particle density and η is called the gas parameter [42]. In current BEC experiments $\eta \leq 10^{-4}$ and $a_s/\lambda_T \leq 10^{-2}$ and thus the pseudo–potential approximation is valid for describing these experiments.

3.2 The Gross–Pitaevskii equation (GPE)

In second quantization the Hamiltonian of the weakly interacting Bose–gas reads

$$H = H_{\mathrm{id}} + \frac{1}{2}\int_{-\infty}^{\infty} d^3x d^3x'\, \Psi^\dagger(\mathbf{x})\Psi^\dagger(\mathbf{x}')V\left(\mathbf{x}-\mathbf{x}'\right)\Psi(\mathbf{x}')\Psi(\mathbf{x}), \tag{20}$$

where according to Sec. 3.1 the interaction potential is given by Eq. (18). We assume the ground state to be of the form

$$|\Phi\rangle = \frac{\left(a_0^\dagger\right)^N}{\sqrt{N!}}\,|\mathrm{vac}\rangle\,, \tag{21}$$

where $|\mathrm{vac}\rangle$ denotes the vacuum state and the creation operator $a_0^\dagger$ is given by

$$a_0^\dagger = \int_{-\infty}^{\infty} d^3x \varphi_0(\mathbf{x})\Psi^\dagger(\mathbf{x}). \tag{22}$$

We want to find the shape of the mode function $\varphi_0(\mathbf{x})$ by minimizing the expression

$$\langle\Phi|\, H - \mu\hat{N}\,|\Phi\rangle \to \min, \tag{23}$$

which after some calculation leads to the Gross–Pitaevskii equation (GPE)

$$\left(-\frac{\hbar^2\nabla^2}{2m} + V_T(\mathbf{x}) + Ng\,|\varphi_0(\mathbf{x})|^2 - \mu\right)\varphi_0(\mathbf{x}) = 0, \tag{24}$$

where $g = 4\pi a_s\hbar^2/m$. This derivation is one of the most intuitive and simple ways to find the GPE. There are several other methods to obtain the GPE which are presented in [23, 43].

In the non–interacting limit $a_s = 0$ the GPE reduces to an eigenvalue equation with the form of a time independent Schrödinger equation for the trap potential $V_T(\mathbf{x})$. This limit agrees with the ideal gas limit Sec. 2, the chemical potential equals the ground state energy ϵ_0 and the mode function $\varphi_0(\mathbf{x})$ is the eigenfunction of the corresponding one particle Hamiltonian. In the opposite limit where the interaction energy dominates the kinetic energy, i.e. $\xi \ll R$ where $\xi = (8\pi a_s N/R^3)^{-1/2}$ is the healing length and R is the size of the condensate cloud, we can neglect the kinetic term [23]. This approximation, called the Thomas–Fermi limit, yields the wave function

$$\varphi_0(\mathbf{x}) = \begin{cases} \sqrt{\frac{1}{Ng}\left(\mu - V_T(\mathbf{x})\right)} & \text{for} \quad \mu > V_T(\mathbf{x}) \\ 0 & \text{for} \quad \mu < V_T(\mathbf{x}) \end{cases}. \tag{25}$$

3.3 The time dependent GPE

Performing the above variational calculation for a time dependent mode function $\varphi_0(\mathbf{x},t)$ yields the time dependent GPE given by

$$i\hbar\frac{\partial}{\partial t}\varphi_0(\mathbf{x},t) = \left(-\frac{\hbar^2\nabla^2}{2m} + V_T(\mathbf{x}) + Ng\,|\varphi_0(\mathbf{x},t)|^2\right)\varphi_0(\mathbf{x},t). \tag{26}$$

The applications of this equation have been studied in [43, 44]. We also want to mention the stability analysis of BEC worked out by S.A. Gardiner et al. in [45] which also makes use of the time dependent GPE.

3.4 The quasiparticle spectrum

Now we want to investigate the quasiparticle spectrum along the lines of [40]. By assuming spontaneous symmetry breaking [46] we write the bosonic field operator as the sum $\Psi(\mathbf{x},t) = \sqrt{N}\varphi_0(\mathbf{x})+\tilde{\Psi}(\mathbf{x})$, where $\varphi_0(\mathbf{x})$ is the condensate wave function and $\tilde{\Psi}(\mathbf{x})$ is assumed to be a small correction. Inserting this into the grand canonical version of the Hamiltonian $K_B = H - \mu\hat{N}$ and neglecting all terms in $\tilde{\Psi}(\mathbf{x})$ higher than quadratic yields

$$\begin{aligned} K_B &\approx \zeta + \int d^3x \tilde{\Psi}^\dagger(\mathbf{x})\mathcal{L}\tilde{\Psi}(\mathbf{x}) + \frac{Ng}{2}\int d^3x \tilde{\Psi}^\dagger(\mathbf{x})(\varphi_0(\mathbf{x}))^2\tilde{\Psi}^\dagger(\mathbf{x}) \\ &+ \frac{Ng}{2}\int d^3x \tilde{\Psi}(\mathbf{x})(\varphi_0^*(\mathbf{x}))^2\tilde{\Psi}(\mathbf{x}), \end{aligned} \tag{27}$$

where ζ is a c–number and

$$\mathcal{L} = \frac{\mathbf{p}^2}{2m} + V_T(\mathbf{x}) - \mu + 2Ng|\varphi_0(\mathbf{x})|^2. \tag{28}$$

This Hamiltonian K_B may be diagonalized by using the Bogoliubov ansatz

$$\tilde{\Psi}(\mathbf{x}) = \sum_j \left(u_j(\mathbf{x})\alpha_j + v_j^*(\mathbf{x})\alpha_j^\dagger\right), \tag{29}$$

where $u_j(\mathbf{x})$ and $v_j(\mathbf{x})$ satisfy the Bogoliubov de–Gennes equations

$$\mathcal{L}u_j(\mathbf{x}) + Ng(\varphi_0(\mathbf{x}))^2 v_j(\mathbf{x}) = E_j u_j(\mathbf{x}), \tag{30}$$

and

$$\mathcal{L}v_j(\mathbf{x}) - Ng(\varphi_0^*(\mathbf{x}))^2 u_j(\mathbf{x}) = -E_j v_j(\mathbf{x}). \tag{31}$$

Up to a c–number the Hamiltonian then reads

$$K_B = \sum_j E_j \alpha_j^\dagger \alpha_j. \tag{32}$$

K_B thus describes a collection of noninteracting quasiparticles for which the condensate is the vacuum.

Starting from this formalism linear response theory can be applied to study the behavior of a BEC under small perturbations and small temperatures $T \ll T_c$. At larger temperatures it is necessary to extend the mean field theory as e.g. in [30, 31, 32] for the effefcts of the thermal cloud.

4 The Bose–Hubbard Model

If a BEC is loaded into an optical lattice the above description in terms of the GPE can become invalid, there might not exist a macroscopic wave function describing the system properly anymore. Here we discuss the extension of the theory for BECs loaded into a deep optical lattice where the condensate character of the BEC can be destroyed. This treatment includes the GPE as a limiting case.

4.1 Optical potential

The optical potential $V_0(x)$ created by the AC-stark shift of two interfering laser beams is given by

$$V_0(x) = (\Omega_0^2/4\delta)\sin^2(kx) \equiv V_0 \sin^2(kx) \tag{33}$$

where Ω_0 is the Rabi frequency and δ the detuning of the lasers from the atomic transition. The laser has a wave number $k = 2\pi/\lambda$ with λ the laser wave length. The periodicity of the optical lattice thus is $a = \lambda/2$. For simplicity we first consider 1D optical lattices. The extension to several dimensions is straightforward and discussed in Sec. 4.9. We expand the optical potential around its minimum to second order

$$V_0(x) \approx \mathcal{C} + \frac{m\omega_T^2 x^2}{2}, \tag{34}$$

with the trapping frequency

$$\omega_T^2 = \frac{\Omega_0^2 \, |\delta| \, k^2}{2\delta^2 m}, \tag{35}$$

and a constant $\mathcal{C}$ that is proportional to the light intensity in the center of the harmonic trap. In a deep optical lattice where the atoms are localized at the potential minima of the optical lattice and hopping between different lattice sites is negligible they will thus be trapped in a harmonic potential with trap frequency ω_T.

4.2 Bloch bands and Wannier functions

The optical potential is periodic in space and it is thus useful to work out the Bloch eigenstates

$$\phi_q^{(n)}(x) = e^{iqx} u_q^{(n)}(x), \tag{36}$$

where q is the Bloch wave number and $u_q^{(n)}(x)$ are eigenstates of the Hamiltonian

$$H_q = \frac{(p+q)^2}{2m} + V_0(x), \tag{37}$$

with energy $E_q^{(n)}$ and periodicity a of the optical potential $V_0(x)$, i.e.

$$H_q u_q^{(n)}(x) = E_q^{(n)} u_q^{(n)}(x). \tag{38}$$

In Figure 3 the bandstructure (eigenenergies $E_q^{(n)}$ as a function of q) is shown for different depths of the optical potential V_0. For the lowest lying bands the separation of the different bands n is approximately given by the frequency ω_T while particles in higher bands with energies larger than V_0 behave as free particles. In the following we assume the particles to be in the lowest band which implies cooling to temperatures T much lower than the trapping frequency ω_T.

4.3 Wannier functions

A set of orthogonal normalized wave functions that fully describe particles in band n of the optical potential and that are localized at the sites (regions around the potential minima) of the optical lattice is given by the Wannier functions [47]

$$w_n(x - x_i) = \mathcal{N}^{-1/2} \sum_q e^{-iqx_i} \phi_q^{(n)}(x), \tag{39}$$

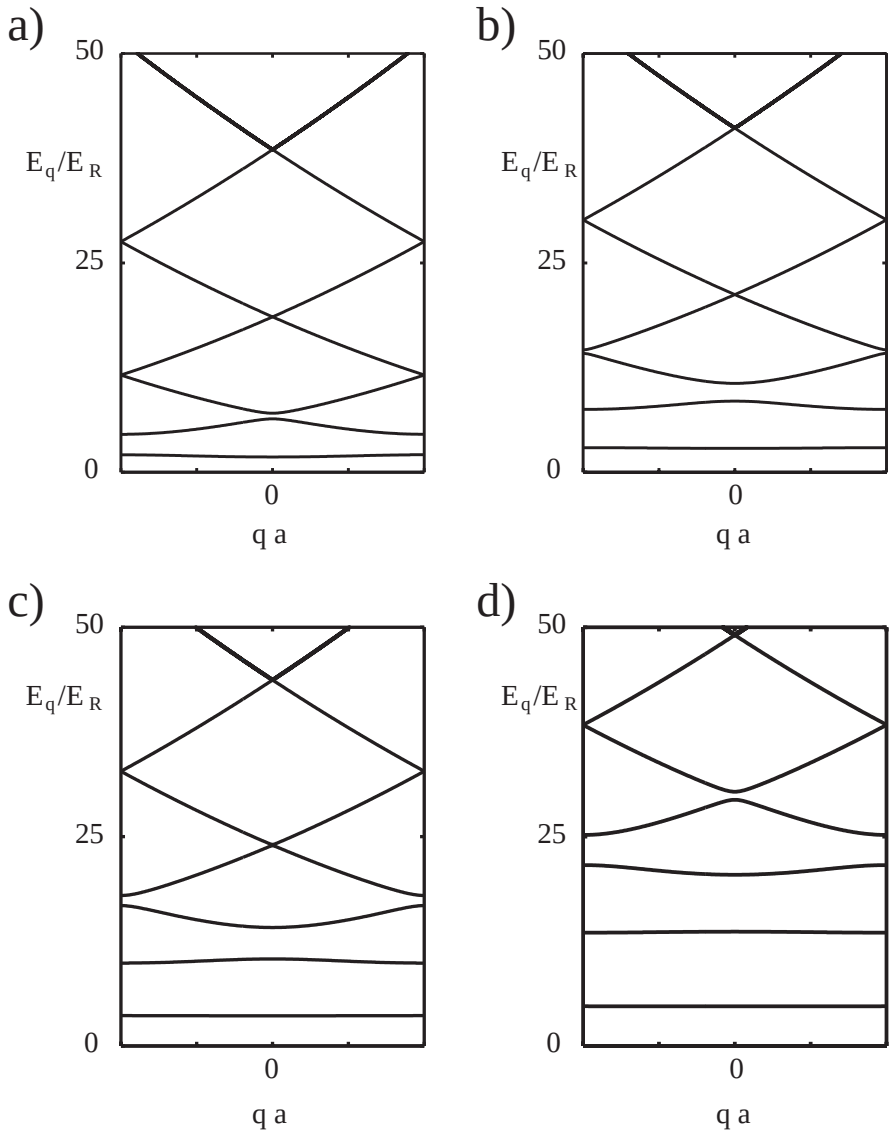

Figure 3: Band structure of an optical lattice with the optical potential $V_0(x) = V_0 \sin^2(kx)$ for different depths of the potential: a) $V_0 = 5E_R$, b) $V_0 = 10E_R$, c) $V_0 = 15E_R$, and d) $V_0 = 25E_R$.

where x_i is the position of the lattice site and $\mathcal{N}$ is a normalization constant. Figure 4 shows an example of a Wannier function with $n = 0$. These Wannier functions $w_0(x - x_i)$ tend towards the gaussian ground state wave function localized in lattice sites with center at x_i when $V_0 \to \infty$ at constant k since we may then neglect all the terms involving the Bloch wave number q and it is valid to approximate the optical potential by a harmonic potential. The advantages of using Wannier functions $w_0(x - x_i)$ to describe particles in the lowest band are that

- a mean position x_i may be attributed to the particle if it is found to be in the mode corresponding to the Wannier function $w_0(x - x_i)$ (cf. Fig. 4) and
- local interactions between particles can be described easily since the dominant contribution comes from particles located at the same position x_i.

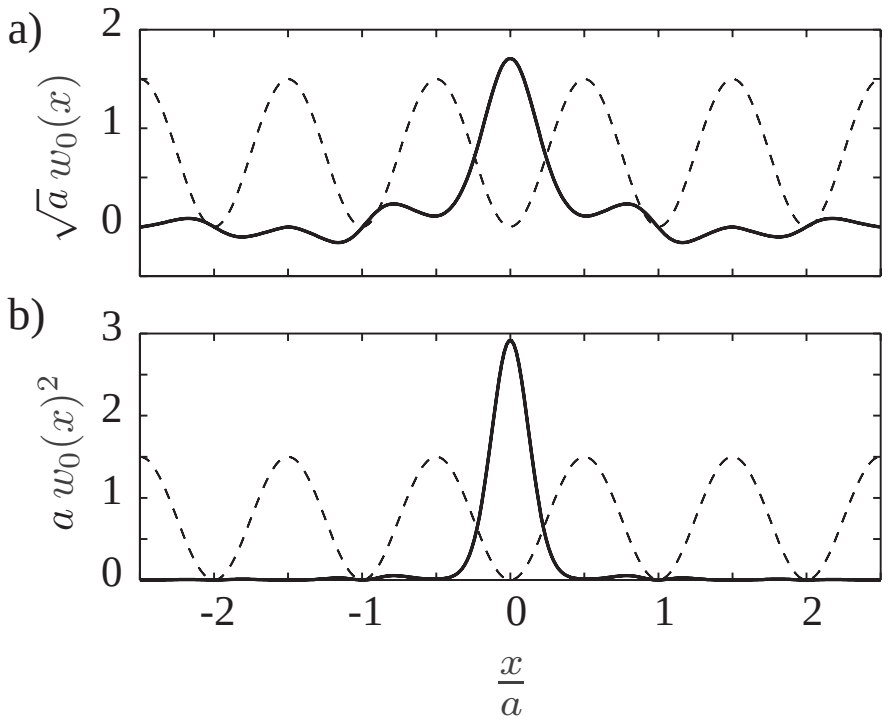

Figure 4: Wannier function for an optical lattice with $V_0 = 10E_R$ (with $E_R = k^2/2m$, the recoil energy). Plot a) shows the mode function $w_0(x)$ (solid curve) and plot b) the probability distribution $w_0(x)^2$ (solid curve) as a function of position x. The dashed curves indicate the shape of the optical potential $V_0(x) = V_0 \sin^2(kx)$.

4.4 GPE for optical lattices

In the case of a weak optical lattice potential where the interaction energy of two particles in a lattice site does not dominate the dynamics and particles can still move easily between the lattice sites the bose gas is well described by a GPE equation where the trap potential is replaced by the sum of magnetic trap and optical lattice potential. By increasing the depth of the lattice the description in terms of a GPE becomes invalid and the following description must be adopted.

4.5 Realizing the Bose–Hubbard Hamiltonian

We will now show how to reduce the Hamiltonian $H_{\rm full}$ of many interacting particles in an optical lattice to the Bose–Hubbard Hamiltonian. We start with

$$\begin{aligned} H_{\rm full} &= \int dx \psi^\dagger(\mathbf{x}) \left(\frac{\mathbf{p}^2}{2m} + V_0(\mathbf{x}) + V_T(\mathbf{x}) \right) \psi(\mathbf{x}) \\ &\quad + \frac{g}{2} \int dx \psi^\dagger(\mathbf{x}) \psi^\dagger(\mathbf{x}) \psi(\mathbf{x}) \psi(\mathbf{x}) \end{aligned} \tag{40}$$

with $\psi(\mathbf{x})$ the bosonic field operator for atoms in the given internal atomic state $|0\rangle$, $V_T(\mathbf{x})$ describes a (slowly varying compared to $V_0(\mathbf{x})$) external trapping potential, e.g. a magnetic trap. g is the interaction strength between the particles. We assume all the particles to be in the lowest band of the optical lattice and expand the field operator in terms of the Wannier

functions $\psi(\mathbf{x}) = \sum_i a_i w^{(0)}(\mathbf{x} - \mathbf{x}_i)$, where a_i is the destruction operator for a particle in site $\mathbf{x}_i$. $w^{(0)}(\mathbf{x} - \mathbf{x}_i)$ is the three dimensional version of the Wannier functions discussed in Sec. 4.3. We find

$$H_{\text{full}} = -\sum_{i,j} J_{ij} a_i^\dagger a_j + \frac{1}{2} \sum_{i,j,k,l} U_{ijkl} a_i^\dagger a_j^\dagger a_k a_l, \tag{41}$$

where

$$J_{ij} = -\int dx w_0(\mathbf{x} - \mathbf{x}_i) \left(\frac{p^2}{2m} + V_0(\mathbf{x}) + V_T(\mathbf{x}) \right) w_0(\mathbf{x} - \mathbf{x}_j) \tag{42}$$

and

$$U_{ijkl} = g \int dx w_0(\mathbf{x} - \mathbf{x}_i) w_0(\mathbf{x} - \mathbf{x}_j) w_0(\mathbf{x} - \mathbf{x}_k) w_0(\mathbf{x} - \mathbf{x}_l). \tag{43}$$

We first compare the interaction matrix element for particles in the same site U_{0000} with the interaction matrix elements for particles in two adjacent sites U_{0101} and the interaction matrix element U_{0001} as shown in Fig. 5a. We find the offsite interaction matrix elements U_{0101} and U_{0001} to be more than one order of magnitude smaller than the onsite interaction matrix element U_{0000} which allows us to neglect offsite interactions. Due to the orthogonality of the Wannier functions hopping is only possible along the x, y and z directions. In Fig. 5b the hopping matrix elements between nearest neighbors J_{01} and between 2nd J_{02} and 3rd J_{03} nearest neighbors (along one of the axes) are compared with each other. For $V_0 > 5E_R$ the latter are at least one order of magnitude smaller than the hopping matrix elements between nearest neighbors and may thus be neglected.

Therefore we arrive at the standard Bose–Hubbard Hamiltonian in the grand canonical ensemble (i.e. we subtract $\mu\hat{N}$)

$$H_{\text{BH}} = -J \sum_{\langle i,j \rangle} a_i^\dagger a_j + \frac{U}{2} \sum_i a_i^\dagger a_i^\dagger a_i a_i + \sum_i (\epsilon_i - \mu) a_i^\dagger a_i, \tag{44}$$

where $J \equiv J_{01}$ and $U \equiv U_{0000}$. The terms ϵ_i arise from the additional (in comparison to the localization of the Wannier functions slowly varying) trapping potential, and are given by

$$\epsilon_i = V_T(x_i). \tag{45}$$

J is called the hopping (tunneling) matrix element for a particle to jump from site x_i to one of the nearest neighbors x_j, and $\langle i, j \rangle$ denotes all pairs of nearest neighbors. The chemical potential μ acts as a Lagrangian multiplier to fix the mean number of particles in the grand canonical case. The repulsive interaction between particles in the same site is described by the interaction matrix element $U > 0$.

4.6 Connection between J and the bandstructure

In the case where $U = 0$ the Hamiltonian H_{BH} Eq. (44) reduces to a tight binding model Hamiltonian. We assume periodic boundary conditions and that the one particle eigenstates of H_{BH} are of the form

$$|\Psi\rangle = \sum_n e^{i\alpha n} a_n^\dagger |0\rangle, \tag{46}$$

with the constant α obeying the equation $\alpha l = 2\pi M$ where l is an integer. The eigenvalue equation for $|\Psi\rangle$ reads

$$H_{BH} |\Psi\rangle = E_\alpha |\Psi\rangle, \tag{47}$$

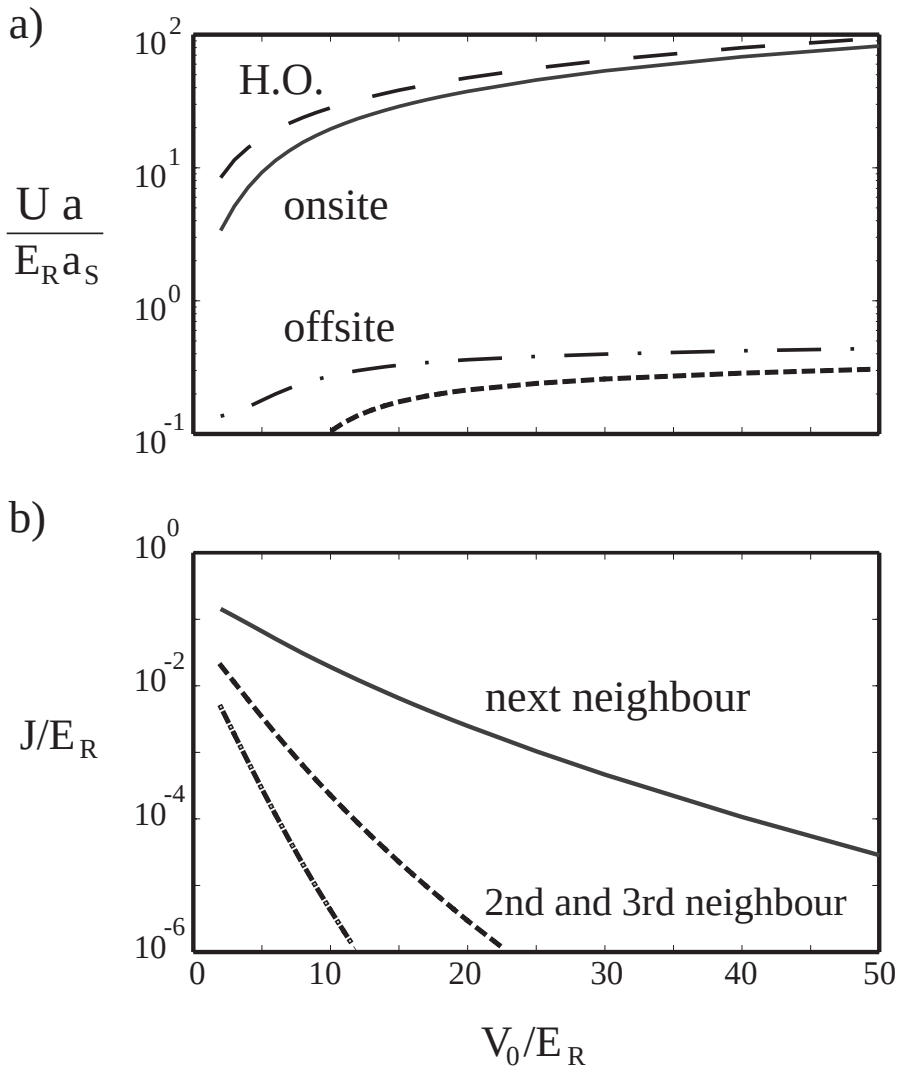

Figure 5: a) Comparison of on site U_{0000} (solid curve) to off site interactions U_{0101} (dash dotted curve) and U_{0001} (dashed curve). The dashed curve labelled HO is the interaction matrix element U_{0000} if the Wannier functions are approximated by the ground state wave function of a harmonic oscillator approximating the optical potential around its minimum. b) Comparison of nearest neighbor hopping J_{01} (solid curve) and hopping to the 2nd J_{02} (dashed curve) and 3rd J_{03} (dash dotted curve) neighbors. All calculations presented in this figure are for a three dimensional optical lattice with equal lattice properties in each direction x, y and z.

from which we find

$$-2J\cos(\alpha) = E_\alpha. \tag{48}$$

From Eq. (48) it is clear that the hopping matrix element is given by

$$J = \frac{\max(E_q^{(0)}) - \min(E_q^{(0)})}{4}. \tag{49}$$

4.7 Approximate ground state

We characterize the ground state of H_{BH} for $\epsilon_i = 0$ for two limiting cases. In the case $U \ll J$ the system is dominated by the kinetic energy and the ground state turns out to be a BEC. In the opposite limit $U \gg J$ the repulsive interaction dominates and the particles are in an insulating ground state.

4.7.1 Limit $U \ll J$

In this case the particles behave almost as if they were free. The ground state is thus approximately given by

$$|SF\rangle \propto (a_1^\dagger + a_2^\dagger + a_3^\dagger \cdots a_M^\dagger)^N |0\rangle \tag{50}$$

(see Fig. 6), where M is the number of lattice sites, N the number of particles, and $|0\rangle$ the vacuum state. This ground state corresponds to a macroscopic occupation of the single particle momentum eigenstate

$$\tilde{a}_k = \frac{1}{\sqrt{M}} \sum_j a_j e^{-ikj} \tag{51}$$

with $k = 0$ of N particles

$$|SF\rangle = (\tilde{a}_0^\dagger)^N |0\rangle \tag{52}$$

and thus to the wave function of a BEC. This kind of state is shown in Fig. 6. In the limit $U = 0$ we obtain excitation energies for the lowest Bloch band $\epsilon_q = J(1 - \cos(qa))$ and therefore the smallest excitation energy $\epsilon_1 \propto J/M^2$ which tends to 0 for large systems $M \to \infty$. The mean particle number in a lattice site is $n_j = N/M$. The fluctuations of the particle number in the ground state in lattice site j is given by

$$\Delta n_j^2 = \langle \psi | a_j^\dagger a_j a_j^\dagger a_j | \psi \rangle - \left(\frac{N}{M}\right)^2 = \frac{N(M-1)}{M^2} \approx \frac{N}{M}. \tag{53}$$

Therefore the particle number fluctuations remain finite for large systems $M \to \infty$.

4.7.2 Limit $U \gg J$

By increasing the repulsive interaction U compared to J a quantum phase transition (at temperature $T = 0$) from the superfluid to a Mott–insulator phase takes place. It becomes less favorable for the particles to jump from one site to the next, since the interaction between two particles in one site increases the energy. For commensurate filling of the sites (i.e. N/M an integer number) the ground state turns into a state where the number of particles per site is integer and the particle number fluctuations tend to zero (see Fig. 6). The ground state is then approximately given by

$$|MI\rangle \propto \prod_{i=1}^{M} \left(a_i^\dagger\right)^{N/M} |0\rangle \,. \tag{54}$$

The lowest excited states can then approximately be written as

$$|n, l\rangle \propto a_n^\dagger \prod_{j \neq l} a_j^\dagger |0\rangle \tag{55}$$

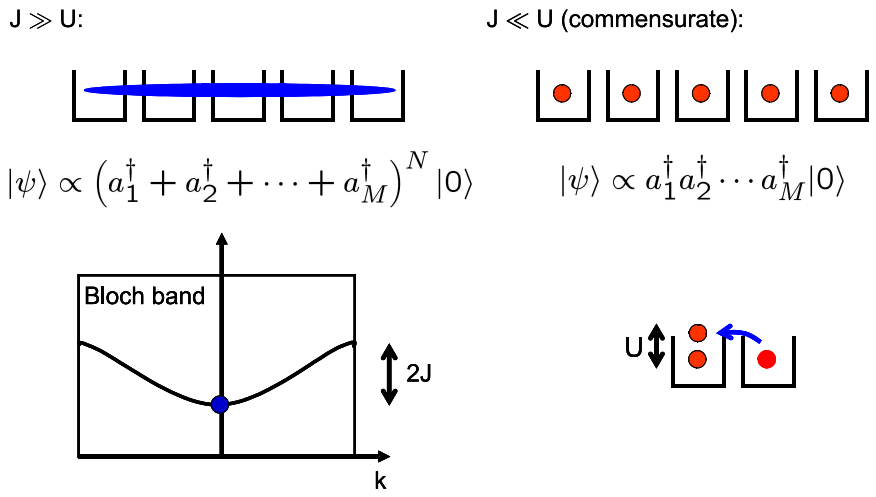

Figure 6: Ground and excited states of H_{BHM} for $J \gg U$ and $J \ll U$.

where $n \neq l$. These have an energy of U independent of the size of the system (gap). For large U the ground state is thus insensitive to perturbations. The mean particle number for $N = M$ per site is then $n_j = 1$ and the fluctuations are

$$\Delta n_j^2 = 0. \tag{56}$$

The ground state is thus isolating, and is called a Mott Insulator (MI) and is shown in Fig. 6. Commensurate filling means that N/M is an integer. Because of its well defined particle number per lattice site and the vanishing particle number fluctuations this MI state is of particular interest for quantum information processing. There MI atoms can function as quantum memory bits (qubits).

4.8 Phase diagram of the Bose–Hubbard model

To give a more quantitative picture of the phase transition described above we will show some results obtained by a Pade analysis by N. Elstner and H. Monien [48] for $\epsilon_i = 0$. The calculations there are carried out for a given chemical potential μ and thus for a fixed mean number of particles corresponding to a grand canonical calculation. In this case the superfluid phase is characterized by a finite order parameter $\langle a_i \rangle \neq 0$ while in the Mott–insulator phase the order parameter $\langle a_i \rangle = 0$ (For a fixed number of particles the order parameter is always zero). Figure 7 shows the phase diagram obtained in [48] for the square lattice in two dimensions. The phase diagram shows the boundary between the Mott–insulator phase and the superfluid phase as a function of J/U and μ/U. The two lobes represent Mott–insulator phases with one and two particles per lattice site, respectively. If the chemical potential is increased further lobes with larger number of particles per lattice site can be found. In [48] the boundary between the superfluid and the Mott–insulator phase is found by calculating the energy difference of particle and hole excitations from a Mott–insulator state $|\Psi_{\mathrm{MIC}}\rangle$. The values of μ/U and J/U where this energy difference vanishes defines the boundary between the two phases (for details see [48, 49]). Using mean field calculations [50] one finds the condition

$$U_c = (3 + 2\sqrt{2})JZ \tag{57}$$

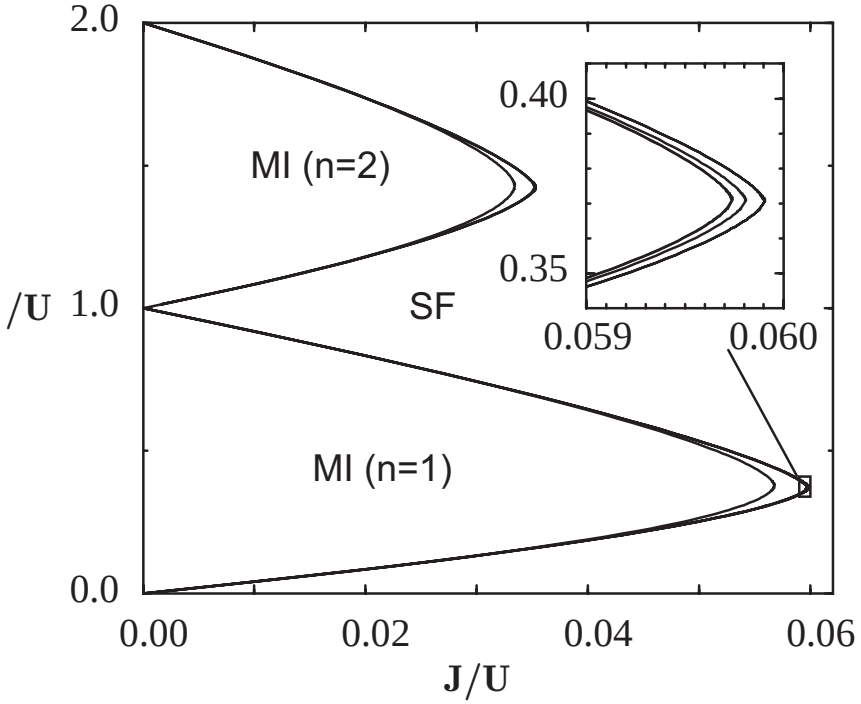

Figure 7: Phase diagram obtained in [48]. The different curves represent different degrees of approximation but are all very close to each other. The calculation was performed for a two dimensional square lattice with $Z = 4$ nearest neighbors.

for the onset of the Mott–insulator phase with one particle per site, where Z is the number of nearest neighbors of one cell. This estimate agrees well with more rigorous calculations like [48].

4.9 One– two– and three dimensional Bose–Hubbard model

The intensities of the laser beams producing the optical potentials in x, y and z direction can be adjusted independently. Also the frequencies have to be adjusted such that the potentials add and do not interfere. Choosing the laser intensity large enough tunneling along different directions can selectively be turned off since the tunneling matrix element decreases rapidly for large V_0 (cf. Fig. 5b). By choosing the laser intensity large along one direction a two dimensional Bose–Hubbard model can be realized whereas by choosing a large laser intensity along two dimensions a one dimensional Bose–Hubbard model is created. The different situations are shown in Fig. 8.

5 Experimental techniques

One of the ultimate goals of laser cooling is to achieve BEC in dilute gases. Due to reabsorption of photons, spontaneous emission and various other heating and loss mechanism this goal has still not been achieved by purely optical methods. Several other experimental techniques for trapping cooling and probing neutral atoms had to be developed to achieve BEC. In this section we will briefly describe the most important of those experimental techniques.

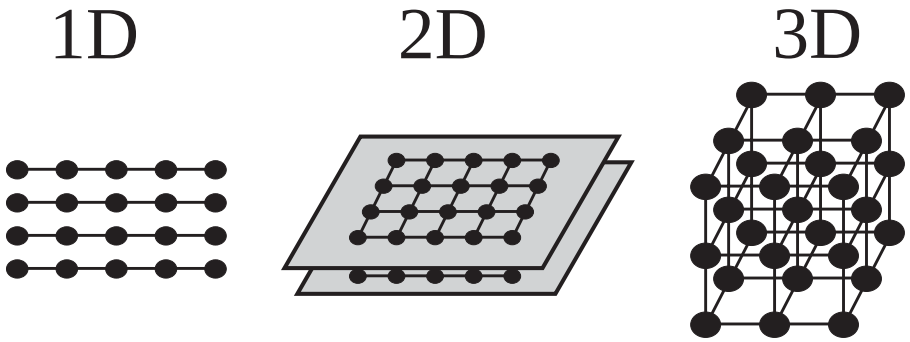

Figure 8: One– two– and three dimensional Bose–Hubbard model. Hopping is only possible along sites connected by lines. In the other directions hopping is turned off by choosing a large laser intensity and thus producing high optical barrier.

5.1 Trapping neutral atoms

The first stage of creating a BEC is usually to load bosonic atoms into a Magneto–Optical–Trap (MOT) and to cool the atoms by Doppler cooling. Then *all* the laser beams are turned off and the precooled sample of atoms is loaded into a purely magnetic trap. There are various different ways to trap neutral atoms in those magnetic traps. They all work in the adiabatic regime where the spin of the atom follows the direction of a (possibly time averaged) magnetic field so that the potential felt by the atoms only depends on the magnitude of the field but not on its direction. One of the difficulties is to avoid Majorana spin flips [51] in positions where the magnetic field is close to zero. The first magnetic trap that allowed trapping of neutral atoms and avoided the spin flips was invented by E.A. Cornell [51]. The zero magnetic field appearing in the center of two anti-Helmholtz coils is moved along a circle by an additional time dependent magnetic field. The time averaged magnetic field felt by the atom is never zero and harmonic around the center. In the first experiments by W. Ketterle and collaborators a blue detuned laser producing a repulsive potential barrier at the center of a magnetic trap was used to prevent the atoms from the region of zero magnetic field [52]. Also several other ways of trapping neutral atoms have been invented like, e.g. the Joffe–Pritchard trap [53]. Later the group by W. Ketterle was even able to load a magnetically trapped BEC into a purely optical trap [5].

5.2 Cooling in magnetic traps

The cooling mechanism used to achieve BEC is evaporative cooling [41]. The trapping potential is truncated at a certain energy value $E_{\rm cut}$ such that only particles with an energy less than $E_{\rm cut}$ can be trapped. Elastic collisions between the atoms trying to bring the gas into thermal equilibrium produce highly energetic atoms with an energy larger than $E_{\rm cut}$. They leave the trap and take away more than the average energy of the trapped particles. The effect is twofold: (i) the temperature of the gas cloud and thus its size shrinks which increases the particle density and (ii) the number of particles and thus the density of the cloud decreases. In order for evaporative cooling to work the effect (ii) has to be smaller than (i) so that the elastic collision rate *increases*. This regime is called runaway evaporation. The conditions necessary to achieve runaway evaporation are described in detail in [41].

We also want to mention that care has to be taken about the so called “bad” collisions. These are the inelastic two and three particle collisions that change the hyperfine levels and lead

to additional loss from the trap and heating. In certain species of atoms, e.g. in Cs inelastic collisions have prevented successful BEC experiments up to now [54].

5.3 Probing a BEC

The experimental techniques on how to measure the properties of a BEC have also undergone some development during the last few years. In the first experiments the BECs were probed by time of flight measurements [55, 56] where the cloud of atoms is released from the trap and allowed to expand for a certain time. After letting the cloud expand, its shape represents the initial velocity distribution [57], and thus by imaging the atom cloud, density and velocity profiles of the condensate can be measured. Note that this technique is destructive.

To allow for multiple measurements on a single condensate the MIT group developed the phase contrast imaging method [58]. Phase shifts in a very far detuned laser beam induced by the refractive index of the condensate are transformed into intensity variations of the laser. The condensate is not destroyed by the far detuned laser beam so that it is possible to perform a sequence of measurements on a single condensate. Also it has become possible to do quantitative non-destructive measurements of the surface area of a condensate [59].

6 Problems

1. **Ideal Bose gas in a power law potential:**

   Consider an ideal Bose gas in 3D trapped by a trapping potential of the form $U(\mathbf{x}) = \kappa r^{3/\delta}$ where κ, δ are constants and r is the distance from the origin. The case $\delta = 3/2$ corresponds to a harmonic oscillator trap and $\delta = 0$ is a box potential.

   The Hamiltonian $\hat{H} = \sum_{i=1}^{N} \hat{h}_i$ of the ideal Bose gas with N particles is given by

   $$\hat{h}_i = \frac{\hat{\mathbf{p}}_i^2}{2m} + \kappa \hat{r}^{3/\delta}. \tag{58}$$

   (i) Calculate the semiclassical approximation to the density of states $\rho(\epsilon)$ of the trapped Bose gas. For which temperatures T may this semiclassical density of states be used for finding the thermodynamic properties of the Bose gas.

   (ii) Find the grand canonical partition function Z_G.

   (iii) Deduce the equation for the number of particles $N(T, Z, \kappa, \delta)$, where $Z = \exp(\mu/k_B T)$ is the fugacity of the system and k_B the Boltzmann constant.

   Remark: For finite particle number N we always have $Z < 1$. How can a thermodynamic limit be defined in this case?

   (iv) Determine the maximum number of particles which can occupy the excited one particle states. Find the critical temperature T_c.

   (v) Show that for very large particle numbers the number of condensate particles is given by

   $$\frac{N_0}{N} = 1 - \left(\frac{T}{T_c}\right)^{3/2+\delta} \tag{59}$$

   for $T < T_c$ and $N_0 = 0$ for $T \geq T_c$ where $N_0 = Z/(1-Z)$ is the number of condensate particles.

   (vi) Numerically find the value of Z for given N and T from the above results. Plot N_0/N as a function of T/T_c for $N = 100, 10^3, 10^7, \infty$ for $\delta = 3/2$ and $\delta = 0$.

   (vii) For $\delta = 3/2$ compare the semiclassical result with exact quantum calculations.

2. **The Gross-Pitaevskii equation (GPE) in 3D:**

   (i) Derive the GPE starting from the Hamiltonian Eq. (20) and the ansatz for the wave function Eq. (21).

   (ii) Discuss the meaning of the healing length and investigate the validity of the Thomas-Fermi approximation.

   (iii) Calculate the ground state wave function for a harmonic oscillator trap potential in Thomas Fermi approximation.

   (iv) Find the dependence of the chemical potential μ on the number of condensate particles.

   (v) Calculate the potential and interaction energy in Thomas Fermi approximation

   (vi) Use the ansatz $\varphi_0(\mathbf{x}) = \sqrt{\rho(\mathbf{x})}\exp(iS(\mathbf{x}))$ for the GPE wave function with real functions ρ and S and find evolution equations for ρ and S from the time dependent GPE. Investigate similarities and difference with hydrodynamics. In which limit is

the quantum pressure term (this is the term that makes the difference between the GPE and hydrodynamics) negligible? What are the properties of the BEC in this case?

3. **Bose-Hubbard model:**

   (i) Starting from Eq. (20) derive the Bose-Hubbard Hamiltonian (BHM) for a potential consisting of a harmonic trap superimposed by an optical lattice.

   (ii) Calculate the ground state of the BHM in the limit $U = 0$ and the opposite limit $J = 0$.

   (iii) Approximate the Wannier functions by ground state wave functions of harmonic oscillators (centered at the potential minima and for frequency ω_T) and calculate the hopping matrix element J and the interaction strength U as a function of the optical lattice depth V_0 for a given scattering length a_s.

References

[1] A. Einstein, Sitzber. Kgl. Preuss. Akad. Wiss., 261 (1924); A. Einstein, *ibid.* 3 (1925).

[2] S.N. Bose, Z. Phys. **26**, 178 (1924).

[3] J.L. Roberts, N.R. Claussen, J.P. Burke, Jr., C.H. Greene, E.A. Cornell, and C.E. Wieman, Phys. Rev. Lett. **81**, 5109 (1998); J. Stenger, S. Inouye, M. R. Andrews, H.-J. Miesner, D. M. Stamper-Kurn, and W. Ketterle, Phys. Rev. Lett. **82**, 2422 (1999).

[4] E.A. Burt, R.W. Ghrist, C.J. Myatt, M.J. Holland, E.A. Cornell, and C.E. Wieman Phys. Rev. Lett. **79**, 337 (1997).

[5] D.M. Stamper-Kurn, M.R. Andrews, A.P. Chikkatur, S. Inouye, H.-J. Miesner, J. Stenger, and W. Ketterle, Phys. Rev. Lett. **80**, 2027 (1998).

[6] D.S. Hall, M.R. Matthews, J.R. Ensher, C.E. Wieman, and E.A. Cornell, Phys. Rev. Lett. **81**, 1539 (1998); D.S. Hall, M.R. Matthews, J.R. Ensher, C.E. Wieman, and E.A. Cornell, Phys. Rev. Lett. **81**, 4531 (1998).

[7] D.S. Hall, M.R. Matthews, C.E. Wieman, and E.A. Cornell, Phys. Rev. Lett. **81**, 1543 (1998); D.S. Hall, M.R. Matthews, C.E. Wieman, and E.A. Cornell, Phys. Rev. Lett. **81**, 4532 (1998).

[8] D.S. Jin, J.R. Ensher, M.R. Matthews, C.E. Wieman, and E.A. Cornell, Phys. Rev. Lett. **77**, 420 (1996); M.-O. Mewes, M.R. Andrews, N.J. van Druten, D.M. Kurn, D.S. Durfee, C.G. Townsend, and W. Ketterle, Phys. Rev. Lett. **77**, 988 (1996); D.S. Jin, M.R. Matthews, J.R. Ensher, C.E. Wieman, and E.A. Cornell, Phys. Rev. Lett. **78**, 764 (1997).

[9] M.R. Andrews, D.M. Kurn, H.-J. Miesner, D.S. Durfee, C.G. Townsend, S. Inouye, and W. Ketterle, Phys. Rev. Lett. **79**, 553 (1997); M.R. Andrews, D.M. Kurn, H.-J. Miesner, D.S. Durfee, C.G. Townsend, S. Inouye, and W. Ketterle, Phys. Rev. Lett. **80**, 2967 (1998).

[10] J. Stenger, S. Inouye, A.P. Chikkatur, D.M. Stamper-Kurn, D.E. Pritchard, and W. Ketterle, Phys. Rev. Lett. **82**, 4569 (1999).

[11] M.-O. Mewes, M.R. Andrews, D.M. Kurn, D.S. Durfee, C.G. Townsend, and W. Ketterle, Phys. Rev. Lett. **78**, 582 (1997); I. Bloch, T.W. Hänsch, and T. Esslinger, Phys. Rev. Lett. **82**, 3008 (1999).

[12] D.M. Stamper-Kurn, H.-J. Miesner, A. P. Chikkatur, S. Inouye, J. Stenger, and W. Ketterle, Phys. Rev. Lett. **81**, 2194 (1998); H.-J. Miesner, D.M. Stamper-Kurn, M.R. Andrews, D.S. Durfee, S. Inouye, and W. Ketterle, Science **279**, 1005 (1998).

[13] E. Hodby, G. Hechenblaikner, S.A. Hopkins, O.M. Marago, and C.J. Foot, Phys. Rev. Lett. **88**, 010405 (2002); F. Chevy, K. W. Madison, V. Bretin, and J. Dalibard, Phys. Rev. A **64**, 031601 (2001); F. Chevy, K. W. Madison, V. Bretin, and J. Dalibard, Phys. Rev. A **64**, 031601 (2001). K. W. Madison, F. Chevy, W. Wohlleben, and J. Dalibard, Phys. Rev. Lett. **84**, 806 (2000)K. W. Madison, F. Chevy, W. Wohlleben, and J. Dalibard, Phys. Rev. Lett. **84**, 806 (2000)

[14] J. R. Abo-Shaeer, C. Raman, J. M. Vogels, W. Ketterle, Science **292**, 476 (2001)J. R. Abo-Shaeer, C. Raman, J. M. Vogels, W. Ketterle, Science **292**, 476 (2001).

[15] B.P. Anderson and M.A. Kasevich, Science 282, 1686 (1998); M. Kozuma, L. Deng, E. W. Hagley, J. Wen, R. Lutwak, K. Helmerson, S. L. Rolston, and W. D. Phillips, Phys. Rev. Lett. **82**, 871 (1999).

[16] D. Jaksch, C. Bruder, J.I. Cirac, C.W. Gardiner, P. Zoller, Phys. Rev. Lett. **81**, 3108; (1998).

[17] M. Greiner, O. Mandel, T. Esslinger, T.W. Haensch, I. Bloch, Nature **415**, 39 (2002).

[18] K. Xu, T. Mukaiyama, J. R. Abo-Shaeer, J. K. Chin, D. E. Miller, and W. Ketterle, Phys. Rev. Lett. **91**, 210402 (2003).

[19] Elizabeth A. Donley, Neil R. Claussen, Sarah T. Thompson, and Carl E. Wieman, Nature **417**, 529 (2002).

[20] C. A. Regal, M. Greiner, D. S. Jin, cond-mat/0401554.

[21] D. Jaksch, H.-J. Briegel, J.I. Cirac, C.W. Gardiner, and P. Zoller, Phys. Rev. Lett. **82**, 1975 (1999).

[22] H.-J. Briegel, T. Calarco, D. Jaksch, J.I. Cirac, and P. Zoller, Journal of Modern Optics **47**, 2137 (2000).

[23] V.L. Ginzburg and L.P. Pitaevskii, JETP **34 (7)**, 858 (1958); L.P. Pitaevskii, JETP **13**, 451 (1961); G. Baym and C.J. Pethick, Phys. Rev. Lett. **76**, 6 (1996).

[24] K. Huang, *Statistical mechanics II* (John Wiley & Sons, Inc., New York); K. Huang and C.N. Yang, Phys. Rev. **105**, 767 (1957); K. Huang, C.N. Yang, and J.M. Luttinger, Phys. Rev. **105**, 776 (1957).

[25] S. Giorgini, L. Pitaevskii, and S. Stringari, Phys. Rev. B **49**, 12938 (1994); F. Dalfovo, S. Giorgini, M. Guilleumas, L. Pitaevskii, and S. Stringari, Phys. Rev. A **56**, 3840 (1997).

[26] J. Javanainen and S. M. Yoo, Phys. Rev. Lett. **76**, 161 (1997); M. Lewenstein and L. You, *ibid.* **77**, 3489 (1997); A. Imamoglu, M. Lewenstein, and L. You, *ibid.* **78**, 2511 (1997); R. Graham, T. Wong, M. J. Collet, S. M. Tan, and D. F. Walls Phys. Rev. A **57**, 493 (1998); Y. Castin and J. Dalibard, Phys. Rev. A **55**, 4330 (1997); J. Javanainen and M. Wilkens, Phys. Rev. Lett. **78**, 4675 (1997); M. J. Steel and D. F. Walls, Phys. Rev. A **56**, 3832 (1997); J. I. Cirac, C. W. Gardiner, M. Naraschewski, and P. Zoller, Phys. Rev. A **54**, R3714 (1996); A. Imamoglu and T.A.B. Kennedy, *ibid.* **55**, R849 (1997); J. Ruostekoski and D.F. Walls, *ibid.* **55**, 3625 (1997); J. Ruostekoski and D.F. Walls, *ibid.* **56**, 2996 (1997).

[27] B. Jackson, J.F. McCann, and C.S. Adams, cond-mat/9907325; T. Winiecki, J.F. McCann, and C.S. Adams, cond-mat/9907224; M. Linn and A.L. Fetter, cond-mat/9907045; A.A. Svidzinsky and A.L. Fetter, cond-mat/9906182 D.L. Feder, C.W. Clark, and B.I. Schneider, Phys. Rev. Lett. **82**, 4956 (1999); P.O. Fedichev and G.V. Shlyapnikov, Phys. Rev. A **60**, R1779 (1999).

[28] P. Öhberg and S. Stenholm, Phys. Rev. A **57**, 1272 (1998); P. Ao and S.T. Chui, Phys. Rev. A **58**, 4836 (1998); S.T. Chui and P. Ao Phys. Rev. A **59**, 1473 (1999).

[29] P.S. Julienne, J. Res. Natl. Inst. Stand. Technol. **101**, 487 (1996).

[30] A. Griffin, Phys. Rev. B **53**, 9341 (1996); A. Griffin, Wen-Chin Wu, and S. Stringari, Phys. Rev. Lett. **78**, 1838 (1997); D.A.W. Hutchinson, E. Zaremba, and A. Griffin, Phys. Rev. Lett. **78**, 1842 (1997).

[31] S. Giorgini, Phys. Rev. A **57**, 2949 (1998).

[32] N. P. Proukakis, K. Burnett, and H.T.C. Stoof, Phys. Rev. A **57**, 1230 (1998); M. Houbiers, H.T.C. Stoof, and E.A. Cornell, Phys. Rev. A **56**, 2041 (1997);

[33] M. Lewenstein, A. Sanpera, V. Ahufinger, B. Damski, A.S. De, U. Sen, Advances in Physics **56**, 243 (2007).

[34] I. Bloch, J. Dalibard, W. Zwerger, Rev. Mod. Phys. (in press), arXiv:0704.3011.

[35] D. Jaksch and P. Zoller, Annals of Physics **315**, 52 (2005).

[36] R.K. Pathria, *Statistical Mechanics*, (Hartnolls Ltd., Bodmin, Cornwall 1996).

[37] P. Nozières in *Bose–Einstein condensation*, edited by A. Griffin, D.W. Snoke, and S. Stringari, (Cambridge University Press 1995).

[38] H.D. Politzer, Phys. Rev. A **54**, 5048 (1996); C. Herzog and M. Olshanii, Phys. Rev. A **55**, 3254 (1997); N.L. Balazs and T. Bergeman, Phys. Rev. A **58**, 2359 (1998).

[39] C.W. Gardiner, M.D. Lee, R.J. Ballagh, M.J. Davis, and P. Zoller, Phys. Rev. Lett. **81** 5266 (1998); H.-J. Miesner, D.M. Stamper-Kurn, M.R. Andrews, D.S. Durfee, S. Inouye, and W. Ketterle, Science **279**, 1005 (1998).

[40] M. Edwards, P.A. Ruprecht, K. Burnett, R.J. Dodd, and C.W. Clark, Phys. Rev. Lett. **77**, 1671 (1996); P.A. Ruprecht, M. Edwards, K. Burnett, and C.W. Clark, Phys. Rev. A **54**, 4178 (1996).

[41] O.J. Luiten, M.W. Reynolds, and J.T.M. Walraven, Phys. Rev. A **53**, 381 (1996); W. Ketterle and N.J. van Druten, Adv. At. Mol. Opt. Phys. **37**, 181 (1996).

[42] Yu. Kagan, G.V. Shlyapnikov, and J.T.M. Walraven, Phys. Rev. Lett. **76**, 2670 (1996).

[43] C.W. Gardiner, Phys. Rev. A **56**, 1414 (1997); Y. Castin and R. Dum, Phys. Rev. A **57**, 3008 (1998).

[44] Yu. Kagan, E.L. Surkov, and G.V. Shlyapnikov, Phys. Rev. A **54**, R1753 (1996); Y. Castin and R. Dum, Phys. Rev. Lett. **77**, 5315 (1996).

[45] S.A. Gardiner *et al.*, preprint.

[46] A.J. Leggett in *Bose–Einstein condensation*, edited by A. Griffin, D.W. Snoke, and S. Stringari, (Cambridge University Press 1995).

[47] C. Kittel, *Quantum Theory of Solids*, John Wiley & Sons, (New York 1963).

[48] N. Elstner and H. Monien, cond-mat/9807033; N. Elstner and H. Monien, cond-mat/9905367.

[49] J.K. Freericks and H. Monien, Phys. Rev. B **54**, 16172 (1996).

[50] A.P. Kampf and G.T. Zimanyi, Phys. Rev. B **47**, 279 (1993); M.P.A. Fisher, P.B. Weichman, G. Grinstein, and D.S. Fisher, Phys. Rev. B **40**, 546 (1989); K. Sheshadri, H.R. Krishnamurty, R. Pandit, and T.V. Ramkrishnan, Europhys. Lett. **22**, 257 (1993); L. Amico and V. Penna, Phys. Rev. Lett. **80**, 2189 (1998).

[51] W. Petrich, M.H. Anderson, J.R. Ensher, and E.A. Cornell, Phys. Rev. Lett. **74**, 3352 (1995).

[52] K.B. Davis, M-O. Mewes, M.R. Andrews. N.J. van Druten, D.S. Durfee, D.M. Kurn, and W. Ketterle, Phys. Rev. Lett. **75**, 3969 (1995).

[53] W. Ketterle, K.B. Davis, M.A. Joffe, A. Martin, and D.E. Pritchard, Phys. Rev. Lett. **70**, 2253 (1993).

[54] J. Söding, D. Guéry-Odelin, P. Desbiolles, G. Ferrari, and J. Dalibard, Phys. Rev. Lett. **80**, 1869 (1998).

[55] M. Anderson, J.R. Ensher, M.R. Matthews, C.E. Wieman, and E.A. Cornell, Observation of BEC in a dilute atomic vapor Science **269**, 198 (1995).

[56] D.S. Jin, J.R. Ensher, M.R. Matthews, C.E. Wieman, and E.A. Cornell, Phys. Rev. Lett. **77**, 420 (1996).

[57] J.R. Ensher, D.S. Jin, M.R. Matthews, C.E. Wieman, and E.A. Cornell, Phys. Rev. Lett. **77**, 4984 (1996).

[58] M.R. Andrews, D.M. Kurn, H.-J. Miesner, D.S. Durfee, C.G. Townsend, S. Inouye, and W. Ketterle, Phys. Rev. Lett. **79**, 553 (1997).

[59] L.V. Hau, B.D. Busch, C. Liu, Z. Dutton, M.M. Burns, and J.A. Golovchenko, Phys. Rev. A **58**, R54 (1998).